ACS APPLIED MATERIALS & INTERFACES

Research Article

www.acsami.org

ZnO Hollow Quantum Dot: A Promising Deep-UV Light Emitter

G. Ouyang*,[†,‡] and G. W. Yang*,[‡]

[†]Key Laboratory of Low-Dimensional Quantum Structures and Quantum Control of the Ministry of Education, Department of Physics, Hunan Normal University, Changsha 410081, Hunan, P. R. China

[‡]State Key Laboratory of Optoelectronic Materials and Technologies, Nanotechnology Research Center, School of Physics & Engineering, Sun Yat-sen University, Guangzhou 510275, Guangdong, P. R. China

ABSTRACT: We establish an analytic model to illustrate the energy bandgap of ZnO hollow quantum dots (HQDs) with negative curvature surface from the perspective of nanothermodynamics. It was found that the bandgap of ZnO HQDs shows a pronounced blue-shift as comparable to those of bulk counterpart and free nanocrystals. Furthermore, the photoelectric properties of ZnO HQDs can be effectively modulated by three independent dimensions, including the outer surface, the inner surface and the shell thickness. Strikingly, the emission wavelength of ZnO HQDs can be extended into the deep-ultraviolet (DUV) region, which suggests this kind of nanostructure could be expected to be applicable for the new-generation, compact, and environmentally friendly alternative DUV light emitter.

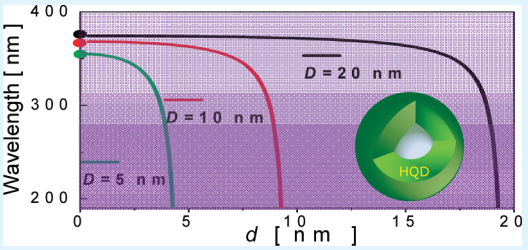

KEYWORDS: *hollow quantum dot, size effect, negative curvature, surface energy, bandgap, deep-ultraviolet*

1. INTRODUCTION

Compact high-efficiency deep-ultraviolet (DUV) solid state light sources have received special attention in recent years because of their intriguing properties from both fundamental scientific issues and potentially industrial applications such as alternatives to toxic, low-efficiency gas lasers and mercury lamps, and in biomedical research, water and air purification, disinfection, and surface modification.[1−7] As reported by Taniyasuand et al.,[2] the emission wavelength from near-band-edge recombination in nitride-based DUV light-emitting diodes (LEDs) is down to 210 nm. Very recently, Fujioka et al.[7] fabricated a flip-chip type DUV LEDs and found the emitting wavelength is 280 nm. Oto et al.[5] further demonstrated the output of 100 mW and a record power efficiency of 40% from $Al_xGa_{1-x}N$/AlN quantum wells emitting at 240 nm using electron-beam pumping technique. These achievements account for the wide-bandgap materials play the crucial role for DUV LEDs and laser diodes.[5,8−10] However, the complicated production technology and the high fabrication cost in AlN- and AlGaN-based structures with quantum-well active layer configuration result in many disadvantages to limit their applications. Therefore, exploring new kinds of compact, robust, and environmentally friendly alternative DUV light sources is of considerable technological interest.

As a wide bandgap (3.37 eV) compound semiconductor with the exciton binding energy of 60 meV, ZnO is environmentally friendly and great potential in applications of UV LEDs, laser diodes, and electroluminescent devices.[11−14] Generally, the UV emission of ZnO is a band-edge emission and corresponds to irradiative recombination of electron from conduction band to hole from valence band. Considering the nanometer size-effect and the quantum confinement,[11,15,16] one could extend the UV emission wavelength of a ZnO nanostructure into the shorter than that of the bulk counterpart. For example, Lin et al.[15] demonstrated that the highly efficient UV emission near band edge of ZnO quantum dots (QDs) shifts to higher energies from 3.0 to 3.43 eV as the QD size decreases from 12 to 3.5 nm. Additionally, Fonoberov et al.[11] found that the origin of UV emission in ZnO QDs is either recombination of confined excitons or surface terminations. Thus, we expect that ZnO not only could be used in the UV emission, but also in the medium-UV and DUV areas. However, this blue-shift of the UV emission wavelength of ZnO QDs is limited at the medium-UV region due to the geometry of QDs, so far.[11,15,16] Therefore, it is really a big challenge whether we could extend the UV emission wavelength of a ZnO nanostructure into the DUV area for the application of ZnO in DUV devices by nanotechnology.

As a new functional nanounit, the nanostructures with negative curvature have attracted considerable interest due to unique properties and potential applications in mesoscopic physics, chemistry and nanodevices.[17] Compared with the nanostructures with positive curvature such as nanoparticles and nanowires, the nanostructures with negative curvature such as hollow nanospheres and nanotubes are more flexible in physical and chemical performances. Therefore, this novel nanostructure can furthest exhibit a variety of nanosized and quantum effects that nanostructures possess, which naturally opens many routes toward new applications.[16,17]

In this contribution, we theoretically demonstrate that the ZnO hollow quantum dot (HQD), a ZnO nanostructure with negative curvature, is a promising DUV light emitter. From the

Received: September 19, 2011
Accepted: December 7, 2011
Published: December 7, 2011

perspective of the nanothermodynamical theory,[17] we establish an analytic model to address the energy bandgap of ZnO HQDs in terms of size-dependent surface energies considerations. Interestingly, we find the bandgap of ZnO HQDs shows a pronounced blue-shift as comparable to those of the bulk counterpart and free nanocrystals. Meanwhile, theoretical analysis unambiguously indicate that the lattice strain induced by surface energy and the uncoordinated atoms in inner of ZnO HQDs with negative curvature and outer with positive curvature surfaces changes the chemical bonding, which leads to a great blue-shift of bandgap. Strikingly, the emission wavelength of ZnO HQDs can be extended into the DUV region, implying that the ZnO HQDs could be expected to be applicable for the DUV light emitter.

2. THEORETICAL MODEL

First of all, we consider the shell−core−shell configuration of a ZnO HQD with N atoms due to a large portion of uncoordinated atoms located in inner and outer surfaces, as shown in Figure 1. Generally, the termination of the lattice

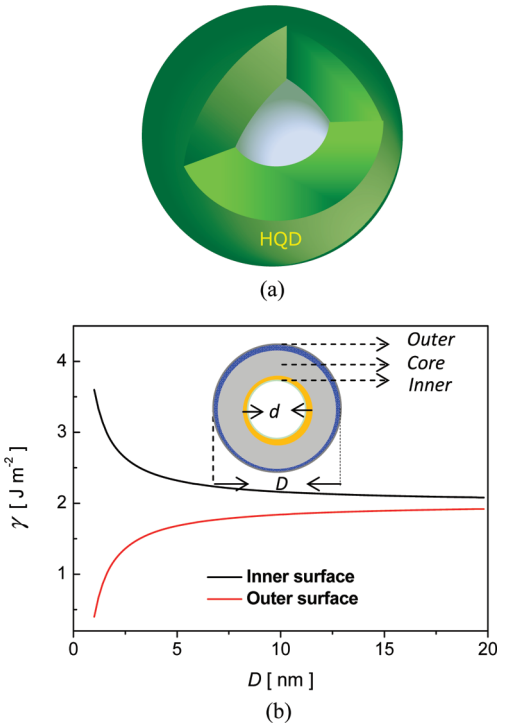

Figure 1. (a) Schematic illustration of a HQD. (b) Size-dependent surface energies in inner and outer surfaces of ZnO HQD. The inset in (b) is the cross section of HQD with shell−core−shell configuration. D and d are the outer and inner diameter, respectively.

periodicity in the two sides of a HQD will lead to excess surface energy. In comparison with a flat surface, the outer surface with positive curvature has lower coordination numbers (CNs), whereas the inner surface with negative curvature has higher CNs. As proposed by the pioneer work of Pauling et al.,[18] the bond length will shrink spontaneously if the CNs of an atom is loss. Furthermore, the single bond strength becomes stronger and the cohesive energy is smaller than that of atoms in the core interior.[19,20] Therefore, the surface energies of two sides of HQDs have a great influence on their properties. Thermodynamically, the surface energy γ is defined as the reversible work per unit area involved in creating a new surface at constant temperature, volume, and total number of moles. In our case, taking into account the total contributions from the chemical part γ^{chem} and the structural part γ^{stru}, the surface energies in inner and outer surfaces of a ZnO QD can be given by[21]

$$\gamma = \gamma^{stru} + \gamma^{chem} \tag{1}$$

It should be noted that the structural part originates from surface strain energy and the chemical part is related surface dangling bond energy. Clearly, the inner surface with negative curvature and the outer surface with positive curvature have different energy state. Thus, we define two surface energies in HQD, i.e., γ_{in} and γ_{out}. Herein, the subscripts with in and out mean the cases in inner and outer surfaces of HQD. Evidently, the inner surface of a HQD is similar with a nanocavity in lattice matrix, whereas the outer surface resembles a free nanocrystal. It is a consequence of considering the reconstruction of surface unit cell, because the self-equilibrium state of nanostructures can be achieved.[22] The bond length d^* in self-equilibrium state of a HQD yields

$$d^* = d_0(1 + \hat{\varepsilon}_{ij}) \tag{2}$$

with

$$\hat{\varepsilon}_{ij} = -\frac{4\gamma}{3DK}\delta_{ij}$$

where d_0, $\hat{\varepsilon}_{ij}$, D, and K are, respectively, intrinsic bond length, self-equilibrium strain, solid size and bulk modulus. The strain in self-equilibrium state can be calculated on the relation: $\hat{\varepsilon}_{ij} = -(1/V_0)C^{-1}_{ijkl}\int_{S_0}\gamma t_{\alpha i}t_{\beta j}dS_0$, in which V_0, C_{ijkl}, t, and S_0 denote volume, elastic constants, transformation matrix and area of a HQD. Assuming the ZnO HQD is an isotropic solid, we can deduce the self-equilibrium strain as $\hat{\varepsilon}_{ij} = -((4\gamma)/(3DK))\delta_{ij}$. Accordingly, the bond contraction coefficients of the atomic layer in inner and outer surfaces are, respectively,

$$c_{in} = 1 - \frac{2\gamma_{in}}{3r_0K} \text{ and } c_{out} = 1 - \frac{2\gamma_{out}}{3RK} \tag{3}$$

where r_0 and R are the inner and outer radii of a HQD.

On the other hand, because of the spontaneous bond contraction in two surfaces of a HQD, the interatomic potential would be perturbed, and resulting in the entire band structure modification. In accordance with our previous considerations,[23] the energy bandgap E_g is proportional to the mean cohesive energy per bond $\langle E_0\rangle$. Thus, we have

$$E_g \propto \langle E_0\rangle \tag{4}$$

and

$$\langle E_0\rangle = \frac{\langle E_{COH}(R, r_0)\rangle}{N\langle z\rangle} \tag{5}$$

with

$$\langle E_{COH}(R, r_0)\rangle = E^B_{COH}(1 + \Delta_D) \text{and} \langle z\rangle = z_b[\tau_{in}(z_{in,b} - 1) + \tau_{out}(z_{out,b} - 1) + 1]$$

where $\langle E_{COH}(R,r_0)\rangle$ is the mean cohesive energy and $\langle z\rangle$ is the mean CNs. Δ_D is the energy perturbation. z_{in}, z_{out}, and z_b are

dx.doi.org/10.1021/am201270r | ACS Appl. Mater. Interfaces 2012, 4, 210−213

the CNs of an atom in inner surface, in outer surface and bulk, respectively.τ_{in} and τ_{out} denote the surface-to-volume ratios in inner and outer surfaces, which are shown as

$$\tau_{in} = \frac{3hV_r}{r_0}\frac{c_{in}}{1 - V_r} \text{ and } \tau_{out} = \frac{3h}{R}\frac{c_{out}}{1 - V_r} \quad (6)$$

Here, V_r represents the ratio between the inner radius and the outer radius, and $V_r = r_0{}^3R^3$. h is the diameter of an atom. Actually, the surface cohesive energy is direct connected with the CNs and $E^S_{COH} = (z_s/z_b)^{1/2}E^B_{COH}$,[24] where E^B_{COH} is the cohesive energy in bulk.

Combining with the eqs 4, 5, and 6, the size-dependent energy bandgap of ZnO HQDs is therefore

$$\frac{E_g(R, r_0)}{E_g(B)} = \frac{z_b}{\langle z\rangle}[\tau_{in}((z_{in,b})^{1/2} - 1) + \tau_{out}((z_{out,b})^{1/2} - 1) + 1] \quad (7)$$

Where $z_{in,b} = z^*_{in}/z_b$,and $z_{out,b} = z^*_{out}/z_b$. Note that z^*_{in} and z^*_{out} are the effective CNs in inner and in outer surfaces after considering the surface effect.

3. RESULTS AND DISCUSSION

Notably, the ZnO HQDs in our case are perfect crystalline without considering the effect of any defects such as points and dislocations. From eq 1, the surface energies in inner and outer surfaces of ZnO HQDs have been calculated, as shown in Figure 1b. It is seen that the surface energy of inner surface increases with decreasing diameter, while the surface energy in outer surface shows the inverse character. If D or d is greater than 5 nm, both surface energies in inner and outer surfaces smoothly go to that of the bulk value. In fact, the most discrepancy is the chemical part of surface energy that it shows the inverse trend in two sides of HQDs.[25] In addition, the structural part of surface energies in inner and outer surfaces becomes larger with decreasing size. Essentially, a large number of surface atoms with lower CNs and higher energetic state due to an increased number of dangling bonds result in the different state compared with the core interior.

Figure 2 describes the mean CNs of entire HQD that it decreases as the size reduction. Also, the thinner shells of

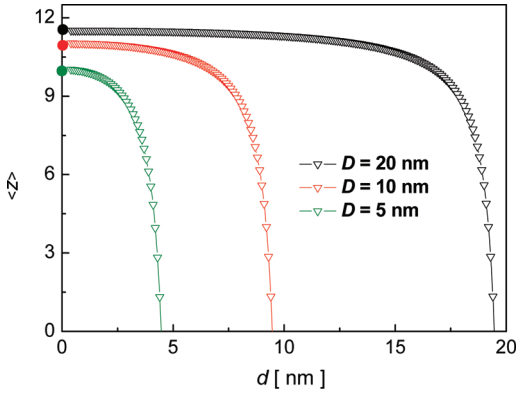

Figure 2. Relationship among the inner and outer diameters and the CNs. The three dots located at the horizontal abscissa mean the cases of QDs.

HQDs have lower CNs than those of the thicker ones. Three dots plotted at the $\langle z\rangle$-axis mean the nanocrystals with 5, 10, and 20 nm without negatively curved surface. Noticeably, compared with free nanocrystals with positive curvature surface, the HQDs with joint effects from both positive surface and negative surface have more complex conditions. Indeed, the most prominent discrepancies among HQD, nanocrystal and their bulk are the significant portion of the uncoordinated surface atoms. Importantly, the local strain will be taken place when the atomic bond length becomes shorter. The self-equilibrium strain in single atomic layer is $\varepsilon = c_i - 1$, which will perturb the crystal potential and further modify the entire band structure.[26] In fact, the lower CNs of nanostructures plays the vital role for many physical quantities, including melting temperature,[27] vacancy formation energy,[28] stiffness,[20] and so on.

Figure 3 shows the size-dependent energy bandgap of ZnO HQDs in terms of eqs 4−7. The bandgap becomes wider with

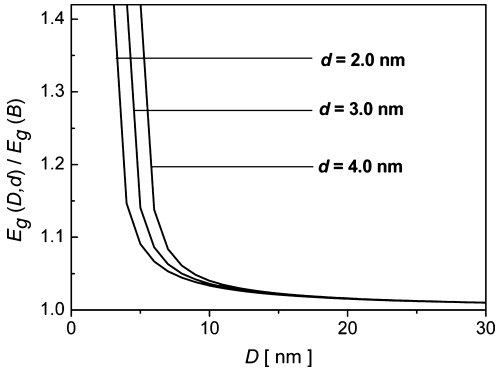

Figure 3. Dependence of bandgap of ZnO HQD on the inner and outer diameter.

decreasing the thickness of quantum shell, implying the confinement effect enhancement in smaller systems. The physical origin is attributed to the size-dependent surface energies in inner and outer surfaces of HQDs. In particular, if $d = 0$ in eq 7, it can be effectively to address the energy bandgap of nanocrystals. In this case, we have

$$\frac{E_g(R)}{E_g(B)} = \frac{z_b}{\langle z\rangle}[\tau((z_{s,b})^{1/2} - 1) + 1] \quad (8)$$

Here $z_{s,b} = z^*_s/z_b$ and $\tau = 3hc/R$. z^*_s is the effective CNs in surface of nanocrystals. Compared with eqs 7 and 8, one can see that the additional term in eq 7 original from the contribution of negatively curved surface is great influence on the energy bandgap, leading to the strong blue-shift of bandgap.

Furthermore, according to the relationship between the emission wavelength and the excitation energy, we speculate on the emission wavelength of ZnO HQDs will extend to the DUV region (C area in Figure 4) if the thickness of spherical shell is up to 1 nm, as shown in Figure 4. Remarkably, three dots located at the λ axis represent the emission wavelength of nanocrystals, which are in the UV region (A area in Figure 4). It is reasonable to conclude that the ZnO HQD is more superior to ZnO nanocrystal for DUV LEDs. We thus believe that ZnO HQDs can be expected as an effective generating DUV light emitter.

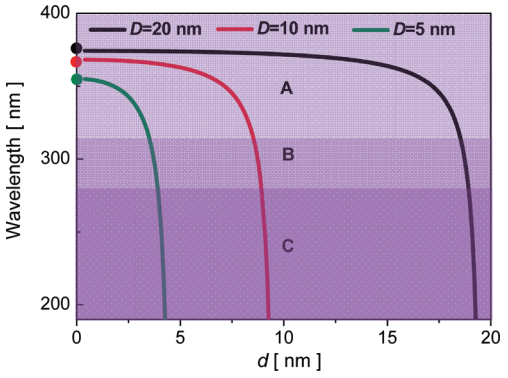

Figure 4. Dependence of emission wavelength of ZnO HQD on the solid size. The A, B, and C denote the three areas of ultraviolet (315−400 nm), medium-ultraviolet (280−315 nm), and deep-ultraviolet (190−280 nm), respectively.

4. CONCLUSION

In summary, based on the size-dependent surface energies consideration, we have theoretically studied the energy bandgap of ZnO HQDs, and indicated that the stronger blue-shift of bandgap in ZnO HQDs as comparable to those of bulk counterpart and free nanocrystals. The underlying mechanism can be attributed to the local strain induced by surface energies and CNs imperfection in inner with negative curvature and outer with positive curvature surfaces of HQDs. Accordingly, these theoretical results were not only new physics about II−IV semiconductor nanostructures but also provided useful information for a next-generation, friendly, compact DUV solid light source.

AUTHOR INFORMATION

Corresponding Author

*E-mail: gangouy@hunnu.edu.cn (G. O.); stsygw@mail.sysu.edu.cn (G.W.Y.).

ACKNOWLEDGMENTS

This work was supported by NSFC (10804030, 11174076, U0734004, and 10974260), Program for Changjiang Scholars and Innovative Research Team in University (IRT0964), Hunan Provincial Natural Science Foundation of China (11JJ7001), Key Project of Chinese Ministry of Education (209088), and Open Fund of the State Key Laboratory of Optoelectronic Materials and Technologies, Sun Yat-sen University (KF2009-MS-09).

REFERENCES

(1) Schubert, E. F.; Kim, J. K. *Science* **2005**, *308*, 1274−1278.
(2) Taniyasu, Y.; Kasu, M.; Makimoto, T. *Nature* **2006**, *441*, 325−328.
(3) Fischer, A. J.; Allerman, A. A.; Crawford, M. H.; Bogart, K. H. A.; Lee, S. R.; Kaplar, R. J.; Chow, W. W.; Kurtz, S. R.; Fullmer, K. W.; Figiel, J. J. *Appl. Phys. Lett.* **2004**, *84*, 3394−3396.
(4) Mayes, K.; Yasan, A.; McClintock, R.; Shiell, D.; Darvish, S. R.; Kung, P.; Razeghi, M. *Appl. Phys. Lett.* **2004**, *84*, 1046−1048.
(5) Oto, T.; Banan, R. G.; Kataoka, K.; Funato, M.; Kawakami, Y. *Nat. Photon.* **2010**, *4*, 767−771.
(6) Taniyasu, Y.; Kasu, M. *Appl. Phys. Lett.* **2010**, *96*, 221110.
(7) Fujioka, A.; Misaki, T.; Murayama, T.; Narukawa, Y.; Mukai, T. *Appl. Phys. Express* **2010**, *3*, 041001.
(8) Khan, A.; Balakrishnan, K.; Katona, T. *Nat. Photon.* **2008**, *2*, 77−84.
(9) Li, J.; Nam, B.; Nakarmi, M. L.; Lin, J. Y.; Jiang, H. X. *Appl. Phys. Lett.* **2003**, *83*, 5163−5165.
(10) Bhattacharyya, A.; Moustakas, T. D.; Zhou, L.; Smith, D. J.; Hug, W. *Appl. Phys. Lett.* **2009**, *94*, 181907.
(11) Fonoberov, V. A.; Balandin, A. A. *Appl. Phys. Lett.* **2004**, *85*, 5971−5973.
(12) Reynolds, D. C.; Look, D. C.; Jogai, B.; Litton, C. W.; Cantwell, G.; Harsch, W. C. *Phys. Rev. B* **1999**, *60*, 2340−2344.
(13) Zhang, L.; Yin, L.; Wang, C.; Lun, N.; Qi, Y.; Xiang, D. *J. Phys. Chem. C* **2010**, *114*, 9651−9658.
(14) Bao, J. M.; Zimmler, M. A.; Capasso, F.; Wang, X. W.; Ren, Z. F. *Nano Lett.* **2006**, *6*, 1719−1722.
(15) Lin, K. F.; Cheng, H. M.; Hsu, H. C.; Lin, L. J.; Hsieh, W. F. *Chem. Phys. Lett.* **2005**, *409*, 208−211.
(16) Lizandara-Pueyo, C.; Siroky, S.; Wagner, M. R.; Hoffmann, A.; Reparaz, J. S.; Lehmann, M.; Polarz, S. *Adv. Funct. Mater.* **2011**, *21*, 295−304.
(17) Ouyang, G.; Wang, C. X.; Yang, G. W. *Chem. Rev.* **2009**, *109*, 4221−4247.
(18) Pauling, L. *J. Am. Chem. Soc.* **1947**, *69*, 542−553.
(19) Sun, C. Q. *Prog. Solid State Chem.* **2007**, *35*, 1−159.
(20) Ouyang, G.; Zhu, W. G.; Sun, C. Q.; Zhu, Z. M.; Liao, S. Z. *Phys. Chem. Chem. Phys.* **2010**, *12*, 1543−1549.
(21) Ouyang, G.; Tan, X.; Yang, G. W. *Phys. Rev. B* **2006**, *74*, 195408.
(22) Ouyang, G.; Li, X. L.; Tan, X.; Yang, G. W. *Appl. Phys. Lett.* **2006**, *89*, 031904.
(23) Ouyang, G.; Sun, C. Q.; Zhu, W. G. *J. Phys. Chem. C* **2009**, *113*, 9516−9519.
(24) Tomanek, D.; Mukherjee, S.; Bennermann, K. H. *Phys. Rev. B* **1983**, *28*, 665−673.
(25) Ouyang, G.; Tan, X.; Cai, M. Q.; Yang, G. W. *Appl. Phys. Lett.* **2006**, *89*, 183104.
(26) Zhu, Z. M.; Ouyang, G.; Yang, G. W. *J. Appl. Phys.* **2010**, *108*, 083511.
(27) Shandiz, M. A.; Safaei, A.; Sanjabi, S.; Barber, Z. H. *Solid State Commun.* **2008**, *145*, 432−437.
(28) Ouyang, G.; Zhu, W. G.; Yang, G. W.; Zhu, Z. M. *J. Phys. Chem. C* **2010**, *114*, 4929−4933.